Computers and Structures 88 (2010) 985–990

Contents lists available at ScienceDirect

Computers and Structures

journal homepage: www.elsevier.com/locate/compstruc

Acoustic displacement tetrahedra developed using the IET rules

S. Correa [a,*], C. Militello [b], M. Recuero [c]

[a] Department of Product Design Engineering, EAFIT University, Medellín, Colombia
[b] Department of Fundamental Physics, Experimental, Electronics and Systems, Universidad de La Laguna, S/C de Tenerife, Spain
[c] Department of Mechanics, School of Industrial Engineers, Universidad Politecnica de Madrid, Madrid, Spain

ARTICLE INFO

Article history:
Received 10 September 2009
Accepted 29 May 2010
Available online 26 June 2010

Keywords:
Fluid–structure interaction
Displacement-based formulation
Spurious modes
Individual element test
Parameterized variational principle

ABSTRACT

A four node, displacement based, acoustic element is developed. In order to avoid spurious rotational modes, a higher order stiffness is introduced. The higher order stiffness is developed from an incompatible strain field which computes element volume changes under nodal rotational displacements fields. The higher order strain satisfies the IET requirements, non affecting convergence. The higher order stiffness is modulated, element by element, with a factor. Thus, the displacement based formulation is capable of placing the spurious rotational modes over the range of physical compressional modes that can be accurately captured by the mesh.

1. Introduction

Acoustic propagation in an inviscid media is generally studied using the pressure p as primitive variable. In doing this, after the finite element approximation, only one unknown per node is obtained. This is a drastic unknown reduction as compared with a displacement based formulation where three unknown displacements u, v, w at each node are necessary to describe the problem. The only drawback in using a pressure formulation can be found when we interface our fluid with an elastic solid or a thin plate. Because they do not share the same variables an equilibrium constraint must be imposed at the boundaries. Then, although an acoustic fluid behaves as an elastic medium, an acoustic fluid element can not be handled by a finite element program like any other structural element. Displacement elements, pressure elements, displacement–pressure mixed and velocity potential have been developed in the past. Refs. [1–9] are, in the authors opinion, the most relevant.

Displacement formulations have been reported by many authors. In formulating these elements following finite element standard procedures, a rank deficient stiffness matrix is obtained. This rank deficiency is not an error; it is due to the fact that strain energy in an acoustic fluid is only computed from volume changes. The displacement field inside the element can compute element shape changes with no volume changes. Any displacement field that describes shape changes without volume variation expands the null space of the stiffness matrix. Those displacements field are called spurious because, although they are consistent with the formulation used, they are not expected in a true irrotational formulation. Moreover, when an eigenfrequency problem is solved the spurious displacements fields combine producing low frequency rotational modes. Many authors [1,8,9] try to catch them by computing the rotational of those fields and adding a fictitious rotational energy. There is not a constitutive equation for such behaviour and a fictitious elastic coefficient must be introduced. It appears in the formulation as a penalty factor. Generally the value of the factor is suggested to be from 1 to 1000 times the compressibility modulus. It is a serious drawback because the results strongly depend on this *a priori* tuning.

In this work a displacement based tetrahedra is proposed. It is not based in a Raviart–Thomas polynomial as the one presented in [10] and neither centerface nor midside degrees of freedom to deal with are necessary. Here an incompatible mode is added in order to make the resulting displacement field irrotational in a weak form. From the resulting incompatible mode a higher order strain is computed. After filtering the higher order strain to satisfy the IET from Bergan [11], a higher order stiffness matrix is built. No rotational measure is introduced and no fictitious elastic coefficient is needed. Nevertheless, a coefficient in front of the resulting higher order stiffness can be introduced. The coefficient can change from element to element without affecting convergence [11,12]. A stabilization strategy is proposed and the coefficient can be computed in closed form as a function of the element size. In this way the spurious modes can be placed over the higher compressional mode that still retains a physical meaning.

* Corresponding author. Tel.: +57 4 2619500x9963; fax: +57 4 2664284.
E-mail address: scorrea5@eafit.edu.co (S. Correa).

0045-7949/$ - see front matter © 2010 Elsevier Ltd. All rights reserved.
doi:10.1016/j.compstruc.2010.05.007

A 3D acoustic cavity and a 3D fluid interaction problem are presented to show convergence, non uniform meshes behaviour and boundary normal definition issues [8,9]. The 3D acoustic cavity is also used to check spurious modes appearance.

2. Constructing the stiffness matrix

2.1. Displacement field and incompatible modes

To describe the displacement field, the same orientation of the coordinate system is assumed for all the elements. Each element uses a system with origin at its center of gravity. In linear tetrahedra the general form for the displacement field is:

$$\mathbf{u}_c = \begin{pmatrix} u_c \\ v_c \\ w_c \end{pmatrix} = \begin{pmatrix} a_1 + a_2 x + a_3 y + a_4 z \\ b_1 + b_2 x + b_3 y + b_4 z \\ c_1 + c_2 x + c_3 y + c_4 z \end{pmatrix} \tag{1}$$

The subscript c stands for the compatible part. The field is linear and the *a, b* and *c* factors can be obtained as a function of the nodal displacements values u_j, v_j, w_j with $j = 1, 2, 3, 4$ and the nodal coordinates [13].

The following incompatible modes are introduced,

$$\mathbf{u}_c = \begin{pmatrix} u_i \\ v_i \\ w_i \end{pmatrix} = \begin{pmatrix} \varsigma g(x,\ y,\ z) \\ \eta g(x,\ y,\ z) \\ \gamma g(x,\ y,\ z) \end{pmatrix} \tag{2}$$

where

$$g(x,\ y,\ z) = zx^2 + xy^2 + yz^2 + xy + yz + zx \tag{3}$$

Constants ζ, η and γ must be determined element by element.

A trial displacement field, $\mathbf{u}^* = \mathbf{u}_c + \mathbf{u}_i$, is constructed in order to obtain ζ, η and γ as a function of the *a, b* and *c* coefficients.

The rotor of the trial field is computed:

$$\nabla \times \mathbf{u}^* = \begin{pmatrix} w^*_{,y} - v^*_{,z} \\ u^*_{,z} - w^*_{,x} \\ v^*_{,x} - u^*_{,y} \end{pmatrix} = \begin{pmatrix} (c_3 + \gamma g_{,y}) - (b_4 + \eta g_{,z}) \\ (a_4 + \varsigma g_{,z}) - (c_2 + \gamma g_{,x}) \\ (b_2 + \eta g_{,x}) - (a_3 + \varsigma g_{,y}) \end{pmatrix} \tag{4}$$

From (4) becomes clear that asking the rotor to cancel at each point inside the element will not produce the desired conditions. Instead the following weak forms are tried:

$$\begin{aligned} &\int_{\Omega_e} (y^2 + z^2)(w^*_{,y} - v^*_{,z}) d\Omega = 0 \\ &\int_{\Omega_e} (z^2 + x^2)(u^*_{,z} - w^*_{,x}) d\Omega = 0 \\ &\int_{\Omega_e} (x^2 + y^2)(v^*_{,x} - u^*_{,y}) d\Omega = 0 \end{aligned} \tag{5}$$

Integrating and rearranging terms, (5) results in the following matrix relationship:

$$\begin{pmatrix} 0 & f_{12} & f_{13} \\ f_{21} & 0 & f_{23} \\ f_{31} & f_{32} & 0 \end{pmatrix} \begin{pmatrix} \varsigma \\ \eta \\ \gamma \end{pmatrix} = \begin{pmatrix} 0 & 0 & 0 & p_{14} & 0 & p_{16} \\ 0 & p_{22} & 0 & 0 & p_{25} & 0 \\ p_{31} & 0 & p_{33} & 0 & 0 & 0 \end{pmatrix} \begin{pmatrix} a_3 \\ a_4 \\ b_2 \\ b_4 \\ c_2 \\ c_3 \end{pmatrix}, \tag{6}$$

which, in compact form becomes:

$$\mathbf{F}\boldsymbol{\psi} = \mathbf{P}\mathbf{d} \tag{7}$$

By nodal collocation a linear relationship can be obtained between vector **d** and the nodal displacements **v** [1]:

$$\mathbf{d} = \mathbf{Q}\mathbf{v} \tag{8}$$

where

$$\mathbf{v}^t = (u_1\ v_1\ w_1\ u_2\ v_2\ w_2\ \ldots\ w_4) \tag{9}$$

Assuming $\mathbf{F}^{-1}$ exists, Eq. (6) shows that $\boldsymbol{\psi}$ will be a null vector for nodal displacements that produces volume changes, because it is independent of a_2, b_3 and c_4, but $\boldsymbol{\psi} \neq 0$ for rotational displacements fields. In this way rotational fields will activate the incompatible modes.

For the sake of simplicity, replacing (8) in (7):

$$\boldsymbol{\psi} = \mathbf{F}^{-1}\mathbf{P}\mathbf{Q}\mathbf{v} = \mathbf{R}\mathbf{v} \tag{10}$$

2.2. The strain measure

In a displacement based acoustic element the only strain measure is the unitary change of volume:

$$e = u_{,x} + v_{,y} + w_{,z} \tag{11}$$

The pressure inside the element is computed as:

$$p = \beta e \tag{12}$$

where β is the compressibility modulus of the fluid. In (12) the continuous mechanics convention is used, that is, a negative change of volume is associated with a negative pressure (stress).

For the element strain two contributions are considered, one from the compatible part of the displacement, e_c, plus a higher order one, e_h, computed from the incompatible modes $\mathbf{u}_i$. The computation of e_h is not straightforward because it follows the recipes presented in [12] in order to satisfy the IET (Individual Element Test).

First, a unitary volume change is computed from the incompatible modes:

$$e_i = \varsigma g_{,x} + \eta g_{,y} + \gamma g_{,z} = \begin{pmatrix} g_{,x} & g_{,y} & g_{,z} \end{pmatrix} \begin{pmatrix} \varsigma \\ \eta \\ \gamma \end{pmatrix} = \mathbf{G}\boldsymbol{\psi} \tag{13}$$

The mean volume averaged strain is computed as:

$$\bar{e}_i = \frac{1}{\Omega_e} \int_{\Omega_e} \begin{pmatrix} g_{,x} & g_{,y} & g_{,z} \end{pmatrix} d\Omega \boldsymbol{\psi} = \bar{\mathbf{G}}\boldsymbol{\psi} \tag{14}$$

Subtracting Eq. (14) from Eq. (13), and recovering Eq. (10), the higher order strain field is obtained:

$$e_h = e_i - \bar{e}_i = (\mathbf{G} - \bar{\mathbf{G}})\boldsymbol{\psi} = (\mathbf{G} - \bar{\mathbf{G}})\mathbf{R}\mathbf{v} \tag{15}$$

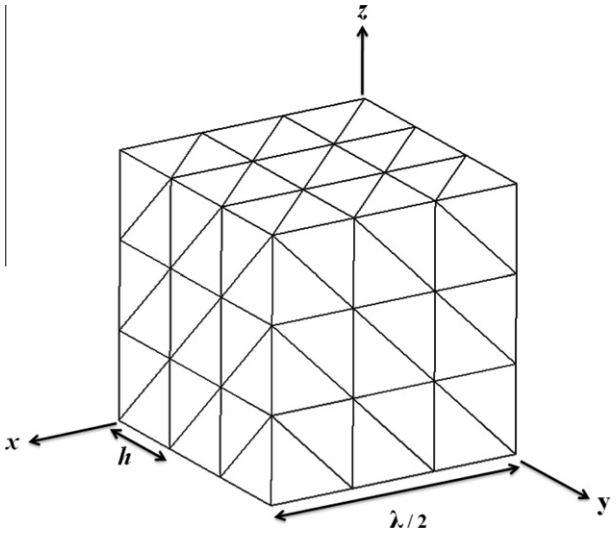

Fig. 1. Sample volume mesh used to compute stabilization coefficient α.

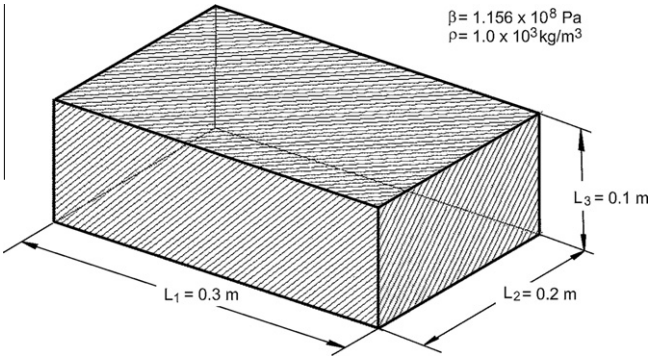

Fig. 2. Rectangular cavity. Dimensions and fluid properties.

Which, in more standard notation,

$$e_h = (\mathbf{G} - \overline{\mathbf{G}})\mathbf{R}\mathbf{v} = \mathbf{B}_h\mathbf{v} \tag{16}$$

From it the higher order stiffness can be computed as:

Table 1
Resonant frequencies for a room with rigid walls. Convergence analysis.

Mesh nodes	1st mode f = 567 Hz	2nd mode f = 850 Hz	3rd mode f = 1022 Hz	4th mode f = 1133 Hz
433	566	849	1023	1127
579	566	848	1020	1127
1719	566	849	1021	1129
1627	566	850	1020	1129

$$\mathbf{K}_h = \int_{\Omega_e} \mathbf{B}_h^t \beta \mathbf{B}_h \mathrm{d}\Omega \tag{17}$$

The basic stiffness is the one in charge to capture the constant strain state, in our case a change of volume, and to produce zero energy under rigid body motions, i.e., translation and rotation. This is achieved using $\mathbf{u}_c$ in the more usual shape function expansion:

$$\mathbf{u}_c = \mathbf{N}^t\mathbf{v} \tag{18}$$

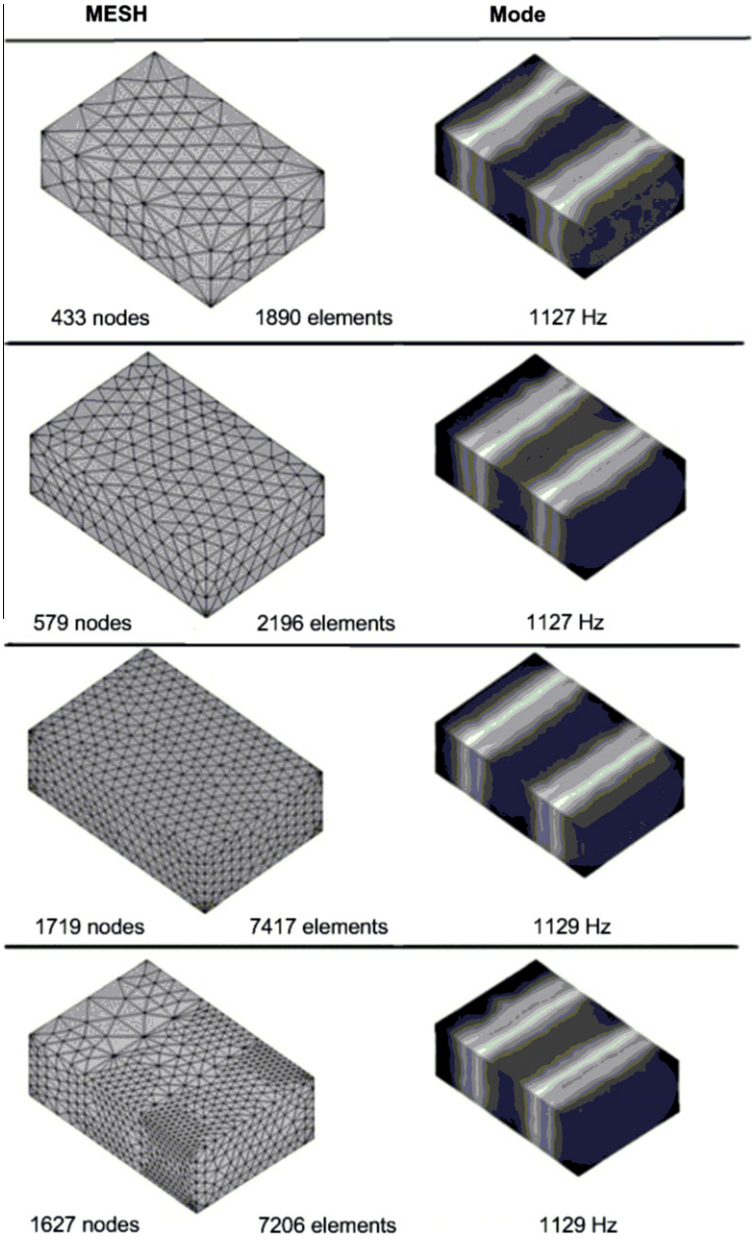

Fig. 3. Rectangular cavity results. Meshes at left. Pressure distribution for the 4th mode at right.

From this displacement field the basic strain field is constructed,

$$e_b = (\,N_{1,x} \quad N_{1,y} \quad N_{1,z} \quad \ldots \quad N_{4,y} \quad N_{4,z}\,)\mathbf{v} = \mathbf{B}_b\mathbf{v} \tag{19}$$

and the basic stiffness is computed,

$$\mathbf{K}_b = \int_{\Omega_e} \mathbf{B}_b^t \beta \mathbf{B}_b \mathrm{d}\Omega \tag{20}$$

The total element stiffness is formed by adding basic and higher order contributions:

$$\mathbf{K}_e = \mathbf{K}_b + \alpha\mathbf{K}_h \tag{21}$$

The value of α can be changed from element to element without affecting the capability of the assembly to correctly capture a constant strain state and rigid body modes. [14].

2.3. Placing the spurious modes at the right place

As stated in the introduction one of the drawbacks of previous formulations is the selection of the penalty factor. A low factor will contaminate the correct modes; a high factor will obscure the contribution of the basic stiffness.

If it is considered that the basic stiffness is in charge to compute the no rotational modes, and it is computed from a linear displacement field, seems reasonable that three elements in a line is the limit to correctly copy half the shortest wavelength. Under these circumstances it is proposed that the energy computed for a rotational mode of the same wavelength should be of the same order that the energy computed for a no rotational mode. To make both energies comparables the eigenfrecuencies are asked to match. The no rotational and rotational displacement fields are:

$$\mathbf{u}_{ir}^t = (\,u_{ir} \quad v_{ir} \quad w_{ir}\,) = \left(\,\sin\left(\tfrac{\pi x}{\lambda}\right) \quad \sin\left(\tfrac{\pi y}{\lambda}\right) \quad \sin\left(\tfrac{\pi z}{\lambda}\right)\,\right) \tag{22}$$

$$\mathbf{u}_r = \begin{pmatrix} u_r \\ v_r \\ w_r \end{pmatrix} = \begin{pmatrix} -\sin\left(\tfrac{\pi x}{\lambda}\right)\cos\left(\tfrac{\pi y}{\lambda}\right)\cos\left(\tfrac{\pi z}{\lambda}\right) \\ -\cos\left(\tfrac{\pi x}{\lambda}\right)\sin\left(\tfrac{\pi y}{\lambda}\right)\cos\left(\tfrac{\pi z}{\lambda}\right) \\ 2\cos\left(\tfrac{\pi x}{\lambda}\right)\cos\left(\tfrac{\pi y}{\lambda}\right)\sin\left(\tfrac{\pi z}{\lambda}\right) \end{pmatrix} \tag{23}$$

They satisfy $\nabla \times \mathbf{u}_{ir} = 0$ and $\nabla \cdot \mathbf{u}_r = 0$.

To compute the value of α in (21) a regular mesh is used, Fig. 1. The displacement fields (22) and (23), are computed at the mesh nodes and the values grouped in vectors $\mathbf{U}_{ir}$ and $\mathbf{U}_r$.

The approximation to the eigenvalue is obtained through the Rayleigh quotient. The mass matrix used in both cases is a lumped diagonal matrix.

$$\omega_{ir}^2 = \frac{\mathbf{U}_{ir}^t \mathbf{K}_b^a \mathbf{U}_{ir}}{\mathbf{U}_{ir}^t \mathbf{M}^a \mathbf{U}_{ir}} \tag{24}$$

$$\omega_r^2 = \alpha \frac{\mathbf{U}_r^t \mathbf{K}_h^a \mathbf{U}_r}{\mathbf{U}_r^t \mathbf{M}^a \mathbf{U}_r} \tag{25}$$

The superscript a indicates that the assembled stiffness for the elements in Fig. 1 is used. It should be noticed that the no rotational field expands the null space of the higher order stiffness matrix, them, α do not contribute to Eq. (24). By the other hand, the rotational field expands the null space of the basic stiffness matrix, so that it does not contribute to Eq. (25). Equating both frequencies the following expression for α is obtained:

$$\alpha = \frac{\mathbf{U}_{ir}^t \mathbf{K}_b^a \mathbf{U}_{ir}}{\mathbf{U}_r^t \mathbf{K}_h^a \mathbf{U}_r} \frac{\mathbf{U}_r^t \mathbf{M}^a \mathbf{U}_r}{\mathbf{U}_{ir}^t \mathbf{M}^a \mathbf{U}_{ir}} \tag{26}$$

The value of α is independent of physical fluid properties. Eq. (26) is computed by constructing a mesh like the one in Fig. 1. The cube side is $\lambda/2$ and the relation between cube side and element side satisfies, roughly:

$$\frac{\lambda}{2} = 3h \tag{27}$$

Cubes are constructed for values of h ranging from 0.01 to 10 m, rotational and no rotational fields for the corresponding λ are computed at the mesh nodes, and finally, Eq. (26) is evaluated. In this way a value of α is computed for each value of h.

The adjusted function for the pairs(α, h), for h in meters is

$$\alpha = \frac{21}{h^2} + 1 \tag{28}$$

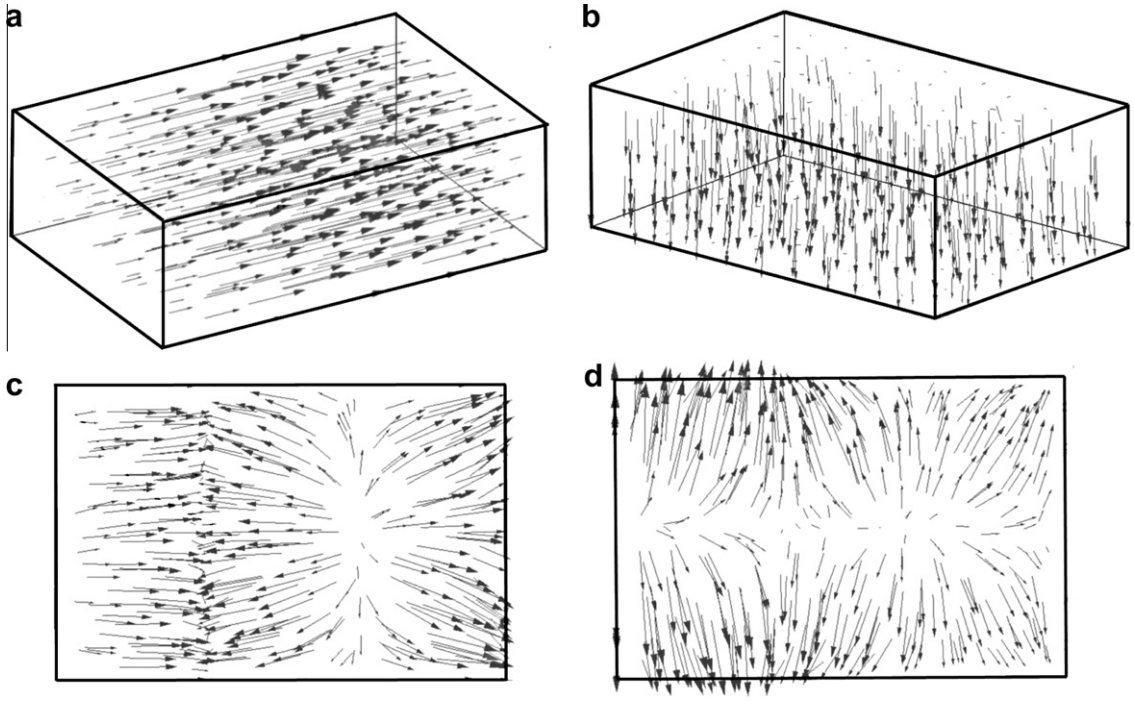

Fig. 4. Spurious modes appearance in a rectangular cavity. (a) First longitudinal mode. (b) First in height mode (6th mode). (c) 7th mode with spurious rotational contamination. (d) 8th mode with a high rotational contamination.

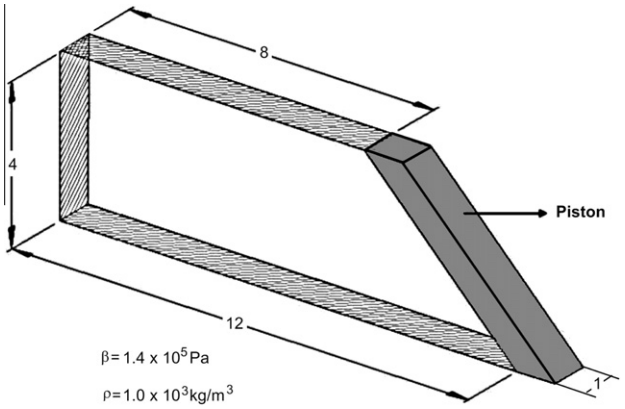

Fig. 5. Skew cavity coupled with piston capable of moving back and forth.

It is surprising that very important changes, of many orders of magnitude, appear for values of h lower than 0.5 m. There is a fast asymptotic convergence to 1 for h greater than 0.5. Eq. (28) is implemented in the program and is computed for each element. To compute the element size h the diameter of a sphere inscribed in the tetrahedra is used. From the point of view of computing α this is conservative because the diameter of the sphere is always smaller than the smallest tetrahedra side.

3. Numerical results

The new formulated element is used to solve two 3D problems in order to assess its performance. One is a closed rectangular cavity and the other is a closed cavity with a skew corner and a rigid moving piston. In both cases convergence respect to the number of equations and effect of discretizing with varying size elements are presented. Because it is a well known fact that normal definition is a concern when imposing impenetrability conditions the piston problem is also run for random perturbations of the interacting surface normal. Four meshes are tried. The last one is constructed with three predominant element sizes.

3.1. Closed rectangular cavity

In a displacement based acoustic element the conditions to be imposed at the rigid walls are impenetrability conditions, i.e., only the displacements perpendicular to the rigid walls are restrained.

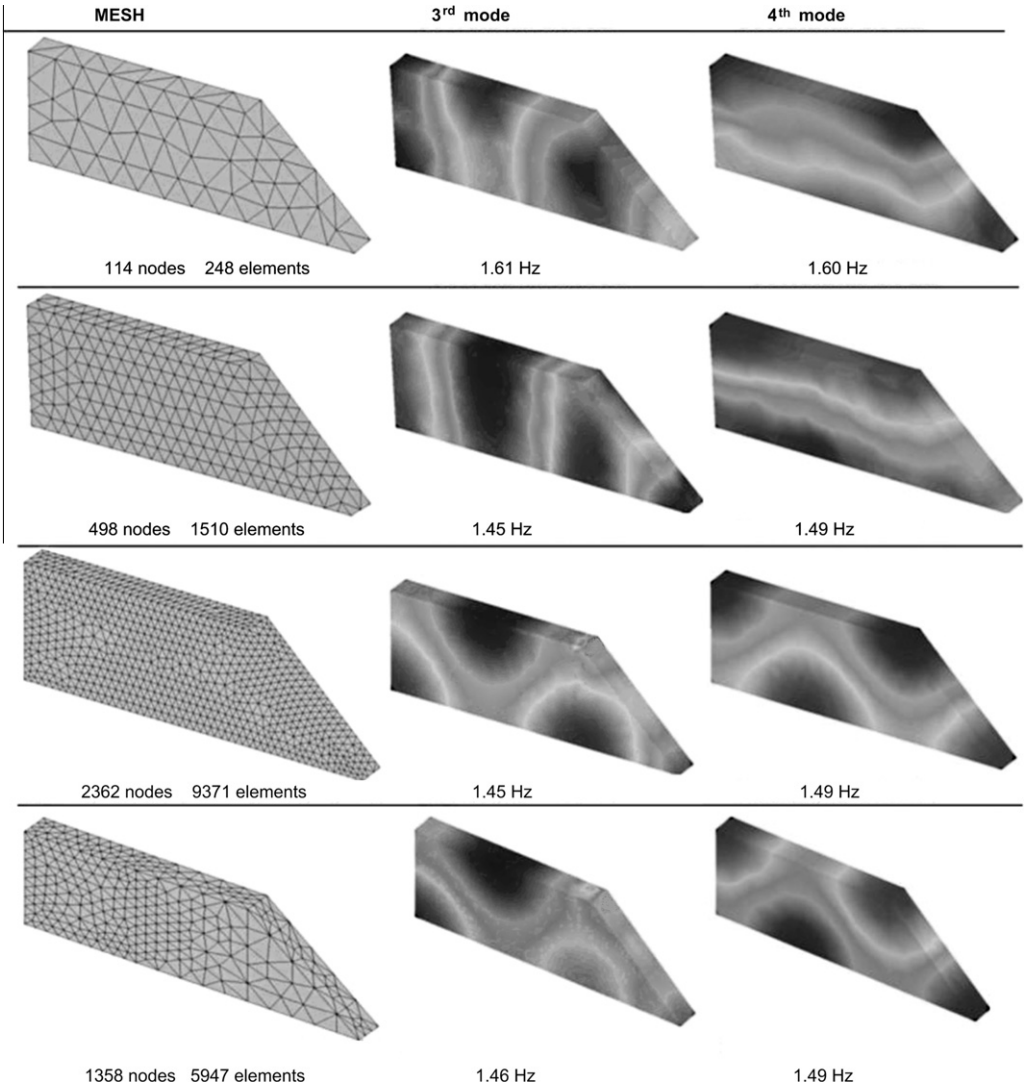

Fig. 6. Skew cavity convergence analysis.

Table 2
Resonant frequencies for the skew cavity with rigid piston. Convergence analysis

Mesh nodes	1st mode $f = 0.29$ Hz	2nd mode $f = 0.88$ Hz	3rd mode $f = 1.45$ Hz	4th mode $f = 1.48$ Hz
114	0.29	0.92	1.61	1.60
498	0.29	0.88	1.45	1.49
2362	0.29	0.88	1.45	1.49
1358	0.29	0.88	1.46	1.49

Table 3
Resonant frequencies for the skew cavity with rigid piston. Convergence analysis with 5° randomly changed interface normals.

Mesh nodes	1st mode $f = 0.29$ Hz	2nd mode $f = 0.88$ Hz	3rd mode $f = 1.45$ Hz	4th mode $f = 1.48$ Hz
114	0.29	0.92	1.61	1.65
498	0.29	0.88	1.45	1.49
2362	0.29	0.88	1.45	1.49
1358	0.29	0.88	1.46	1.49

The fluid properties and dimensions are shown in Fig. 2. The eigenfrequencies can be computed from

$$f[\mathrm{Hz}] = c\pi\sqrt{\left(\left(\frac{l}{L_1}\right)^2 + \left(\frac{m}{L_2}\right)^2 + \left(\frac{n}{L_3}\right)^2\right)} \quad \text{where } l,\ m,\ n = 0,\ 1,\ 2,\ 3,\ldots \tag{29}$$

Four meshes, coarse, medium and refined plus a mesh with three predominant element sizes, are presented in Fig. 3 left. The modal pressure distribution for mode 4 is shown at the right side. In Table 1 convergence to the first 4 modes is shown.

3.1.1. Spurious mode appearance

Looking at the coarse mesh in Fig. 3 and taking into account the stabilization procedure proposed, the first spurious mode must show up after the first half wave in the height direction is computed. Fig. 4a shows the displacement vectors for the first mode, longitudinal, with maximum amplitude at middle length. All of them are parallel to the longitudinal walls. Fig. 4b shows the 6th computed mode. It is the first one in the height direction. Fig. 4c shows the results for the 7th mode. Supposed to be a longitudinal one, some rotational circulating vectors appear. In Fig. 4d the 8th mode has a high content of a rotational field. Looking at the mesh, the 6th mode is the last one to be captured by using three elements in half wavelength. Although it is not conclusive, it seems that the spurious modes appeared in a convenient place. For many others problems run by the authors this has been the case and no contamination had shown.

3.2. Skew cavity with rigid piston

A well known fluid–structure interaction problem [8] is presented in Fig. 5. Fig. 6 shows the meshes and the results obtained for the 3rd and 4th modes. In Table 2 the convergence results are shown. It is interesting for this problem to notice the pressure modes obtained for the 3rd and 4th mode, 1.45 and 1.49 Hz, respectively. A coarse mesh captures a longitudinal and a transversal mode respectively. A fine mesh captures for both frequencies a linear combination of the previous ones. The last one is the represented in [8]. The eigensolver is Eispack trough the Matlab interface [15].

For the interface piston–fluid the normal is randomly perturbed 5°. The effect in convergence is shown in Table 3.

4. Discussion and conclusions

The present element is a three dimensional one and its degrees of freedom can be easily matched with solid elements and plates. Although it has a free parameter, an energy balance allows having it in a closed form, built in inside the software. It is element size dependent and it does not influence element convergence. It is much better than a factor that has to change between 1 and 10,000 times the compressibility factor, depending on the problem.

Convergence is good, it seems insensible to a reasonable error in normal definition and it also shows and excellent behaviour in the fluid–piston interaction problem.

The spurious modes do not disappear, as in a Raviart–Thomas formulation, but the factor manages to put them over the last compression mode that the mesh can catch accurately.

And at last, the Free Formulation, the IET and the parametrized variational principles, PVP, can be used for something more than structural elements.

Acknowledgements

Carmelo Militello would like to thank Professor Carlos Felippa for teaching him. Thanks again. Santiago Correa would like to thank Professor Carmelo Militello for doing the same.

References

[1] Hamdi MA et al. A displacement method for the analysis of vibrations of coupled fluid–structure systems. Int J Num Meth Eng 1978;13:139–50.
[2] Belytschko TB, Kennedy JM. A fluid–structure finite element method for the analysis of reactor safety problems. Nucl Eng Des 1976;38:71–81.
[3] Belytschko TB. Fluid–structure interaction. Comput. Struct. 1980;12:459–69.
[4] Morand H, Ohayon R. Substructure variational analysis of the vibrations of coupled fluid–structure system. Finite element results. Int J Num Meth Eng 1979;14:741–55.
[5] Everstine GC. A symmetric potential formulation for fluid–structure interaction. J Sound Vib 1981;79:157–60.
[6] Olson LG, Bathe KJ. Analysis of fluid–structure interactions. A direct symmetric coupled formulation based on the fluid velocity potential. Comput Struct 1985;21:21–32.
[7] Felippa CA, Ohayon R. Mixed variational formulation of finite element analysis of acoustoelastic/slosh fluid–structure interaction. J Fluid Struct 1990;4:35–57.
[8] Bathe KJ, Nitikitpaiboon C, Wang X. A mixed displacement-based finite element formulation for acoustic fluid–structure interaction. Comput Struct 1995;56:225–37.
[9] Wang X, Bathe KJ. Displacement/pressure based finite element formulations for acoustic fluid–structure interactions. Int J Num Meth Eng 1997;40:2011–7.
[10] Bermudez A, Rodriguez A. Finite element computation of the vibration modes of a fluid–soil system. Comp Meth Appl Mech Eng 1994;119:355–70.
[11] Bergan PG, Hanssen L. A new approach for deriving "good" finite elements. In: Whiteman JR, editor. The mathematics of the finite element, vol. II. London: Academic Press; 1975.
[12] Militello C, Felippa CA. The individual element test revisited. In: Oñate E et al., editors. The finite element in the 1990s. Springer-Verlag; 1991.
[13] Zienkiewicz OC, Taylor RL. The finite element method. The basis, vol. I. Oxford: Butterworth-Heinemann; 2000.
[14] Felippa CA, Militello C. Variational formulation of high performance finite elements: parametrized variational principles. Comput Struct 1990;36:1–11.
[15] MATLAB. The language of technical computing. Version 6.5, 2002.